Volume 19, Issue 4, 192537 (1-11)

Journal of Theoretical and Applied Physics (JTAP)

https://doi.org/10.57647/j.jtap.2025.1904.37

Impact of non-thermal plasma on radish seeds using plasma jet at atmospheric pressure

Bablu Kant Thakur[1], Rajendra Shrestha[2,3,*], Arun Kumar Shah[3], Ram Lal Shah[4], Reeta Silpakar[5], Lekha Nath Mishra[2,*]

[1] *Department of Physics, Trichandra Multiple Campus, Tribhuvan University, Kathmandu, Nepal.*
[2] *Department of Physics, Nepal Banepa Polytechnic Institute, Banepa, Kavre, Neapl*
[3] *Department of Physics, Patan Multiple Campus, Tribhuvan University, Lalitpur, Nepal.*
[4] *Department of Physics, Padmakanya Multiple Campus, Tribhuvan University, Kathmandu, Nepal.*
[5] *Department of Information Technology, Nepal Banepa Polytechnic Institute, Banepa, Kavre, Neapl.*

[*] **Corresponding authors:** rajendra.ts2002@gmail.com, lekha.mishra@pmc.tu.edu.np

Original Research
Received:
29 April 2025
Revised:
20 June 2025
Accepted:
14 August 2025
Published online:
31 August 2025

Abstract:
Using a plasma jet at ambient temperature and atmospheric pressure, the investigation was conducted to determine the potential effects of non-thermal plasma on radish seeds. A cold atmospheric plasma jet with an argon gas source was employed for this system. Six treatment dose and one control were utilized to measure the germination parameters. The impact of atmospheric pressure plasma on treated radish seed germination over several time periods was observed under a working voltage 5 kV, and an argon flow rate 2 L/min. The germination percentage, and shoot length were all boosted at an ambient condition. The optimal germination appears to be two minutes of operating time whereas it reduces for 2.5 and 3 minutes. Both untreated and plasma-treated seeds were characterized using Fourier Transform Infrared Spectroscopy. Radish leaves' chlorophyll content was measured and it is revealed that the treated seeds have more chlorophyll. Electrical and optical techniques have been used to create and characterize the plasma jet.

Keywords: Ambient temperature; Argon gas; Germination; Shoot length; Chlorophyll

1. Introduction

Along with solid, liquid and gas, plasma is the fourth state of matter which is composed of highly energetic positively charged ions, electrons and neutrals [1]. During generation of plasma, the gas is allowed to pass into the system which is ionized by electric current. The significant heat is produced because of electrical resistivity due to which electrons strips away from the gas molecules, forms ionized gas stream called plasma [2]. The plasma technique can be classified into two categories based on temperature of plasma: Thermal plasma and non-thermal plasma [3].
The thermal plasma is produced at high pressure where all gas particles are strongly ionized and that of plasma has high temperature ranges 4000 K to 20000 K [4]. The thermal plasma is widely used in material processing, coating technologies, slag metallurgy, synthesis of powders [5]. Non-thermal plasma is also known as cold atmospheric plasma because of its low temperature. Cold atmospheric plasma utilizes very few electrical energies and can generate plasma at atmospheric pressure [6].
Cold atmospheric pressure plasma plays a crucial role in medication for microorganism decontamination in industrial purposes for increasing surface hydrophilicity [7, 8]. Not only this, but also, cold atmospheric pressure plasma is widely used in technological and biomedical field [9–11]. The plasma treatment causes a surface functionality that affect surface properties due to which wetting behavior of the surface gets modified [12–14]. The plasma treatment creates roughness of the surface which changes wettability of the surface [15]. Cold atmospheric pressure plasma treatment increases wettability, implicity and water absorption [16]. Cold atmospheric pressure plasma uses for decontamination of grams and vegetable seeds, [17, 18] enzyme activity [19, 20] and yield of plants [21]. Cold atmospheric pressure plasma causes less damage to the seeds because

active substances penetrate into the seeds to several nanometers [22, 23].

Radish (Raphanus Sativus L.) is a vegetable cultivated in large quantities worldwide. It has a large succulent hypocotyl [24]. Radish is cultivated in large quantities due to its beneficial properties for humans. Radish is vegetable of Brassicaceae family which is consumed worldwide because of its nutritional value [25, 26]. Radish is classified into two groups according to the season i.e. spring-summer and winter in which crops are grown [27]. It is a good source of potassium, magnesium, calcium, manganese, copper, Vitamin B_6, and Vitamin C [28]. It is found that cold plasma significantly increased seed germination. The seed germination was increased by plasma treatment on radish seeds [29].

It has been shown that the effect of plasma on the surface causes the enhancement of surface, hydrophilicity, which promote seedling growth. The suitable processing condition may be different for different discharge conditions, however, the longer treatment time on seeds can damage its surface [30].

2. Materials and methods

Two bundles of radish were collected from the market. Each packet contains about 200 seeds. After that, fifty radish seeds were kept in a petri dish and was exposed to the plasma for varying periods of time. These seeds, both treated and untreated, were planted in a seed tray with 50 cells. One seed was planted in each cell. Every morning, $15-20$ mL water was injected into each cell through a syringe and the germination rate was also recorded.

2.1 Experimental setup

The Cold Atmospheric Pressure Plasma Jet was used to plasma treat the radish seedlings. Argon gas, dielectrics, electrodes, a voltage controller, and a high voltage power source make up the cold atmospheric pressure plasma jet. In place of the costly RF power supply, the high voltage power supply is used. The output of the power supply is 4 kV, 30 mA, and 29 kHz. 220 V is linked to this high voltage power supply's input. 3 mm was the internal diameter of the copper electrode. An electrical supply was connected to the copper electrode. The nozzle tip was 4 mm from the ground electrode, and the spacing between two electrodes was set at 60 mm. Fig. 1 displays the schematic diagram of the experimental setup.

The argon gas flow rate was kept constant at 2 L/min. By monitoring the current and voltage waveforms and analyzing them with a TEKTRONIX TDS 2002 oscilloscope and a current and voltage probe (PINTEX HVP-28HF), respectively. As a result, electrical characterization of the discharge was completed. The voltage probe's attenuation ratio is 1000:1. Using an optical emission spectrometer, the discharge was optically characterized using the stark broadening method and the line intensity ratio method. The HR1 High Resolution Spectrometer (ASEQ instruments) served as the OES. The $200-830$ nm detection range was used. 300 gr/mm grating element, 0.176 nm resolution, and 10 micron slit width.

Using a PIKE technologies spectrometer, the ATR-FTIR spectroscopic measurements of the seed were carried out in the $4000-450$ cm^{-1} spectral band, with a resolution of 4 cm^{-1}, a scan speed of 0.2, and an accessory type MIRACLE.

The chlorophyll of radish leaves was measured by chlorophyll meter TYS-B DZEO9.

Figure 1 and Fig. 2 depict the plasma jet schematic diagram and the seed treatment by plasma jet, respectively.

3. Result and discussion

3.1 Electrical characterization of plasma jet

The electron density in the glow phase of discharge is calculated using power-balanced approach. The discharge is dispersed across the whole region while in the glow mode. Consequently, the power balance approach is appropriate for estimating electron density. The energy received by plasma

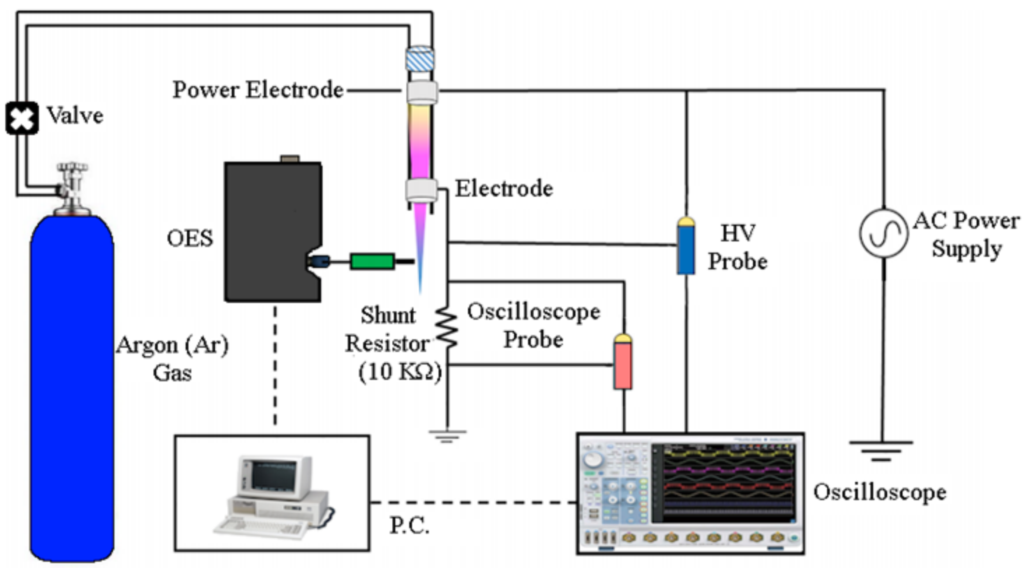

Figure 1. Schematic diagram of the plasma jet.

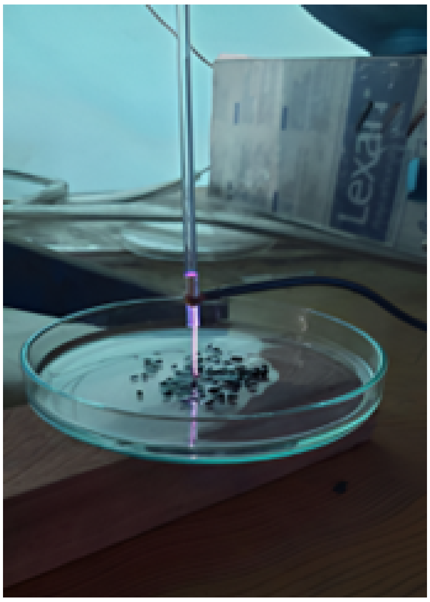

Figure 2. Seed treatment by plasma jet.

from the plasma source and the energy lost by plasma components are balanced in this manner [31–33]. The typical voltage and current waveform over time, where several micro-discharges occur, is depicted in Fig. 3. It turns out that current is more variable than voltage, meaning that current fluctuates more than voltage. Because of this, our high voltage power supply's capacitive load of APPJ is greater than its inductive load. Furthermore, current variation is caused by current leakage.

The electron density was calculated by using power balance method.

$$n_e = \frac{P_{av}}{2AV_bE_{lost}} \tag{1}$$

where $P_{av} = VI$ is the average power dissipation, area of electrode $(A) = 28.2 \times 10^{-6}$ m^2, Bohm velocity $(V_b) = 2 \times 10^3$ m/s, energy lost $(E_{lost}) = 50$eV $= 80 \times 10^{-19}$ J, applied voltage $(V) = 7$ kV, discharge current $(I) = 16.5$mA $= 16.5 \times 10^{-3}$ A, the electron density was found to be 1.28×10^{17} m^{-3}.

Lissajous figures are frequently used to determine the power utilized when utilizing a sinusoidal bias voltage difference. For plasma jet arrangement, the Lissajous figure often takes the form of a parallelogram. [Bigahzoli, U. et al.] The power lost in the cold atmospheric pressure plasma is determined by using $P = f\int V(t)I(t)dt$, where f is frequency. The Lissajous figure obtained is in parallelogram shape, which is shown in Fig. 4. From Lissajous figure and voltage and current waveform characteristics, it is found that the energy dissipated and power consumed in discharge per cycle is 3.331×10^{-4} J and 6.662 Watts respectively.

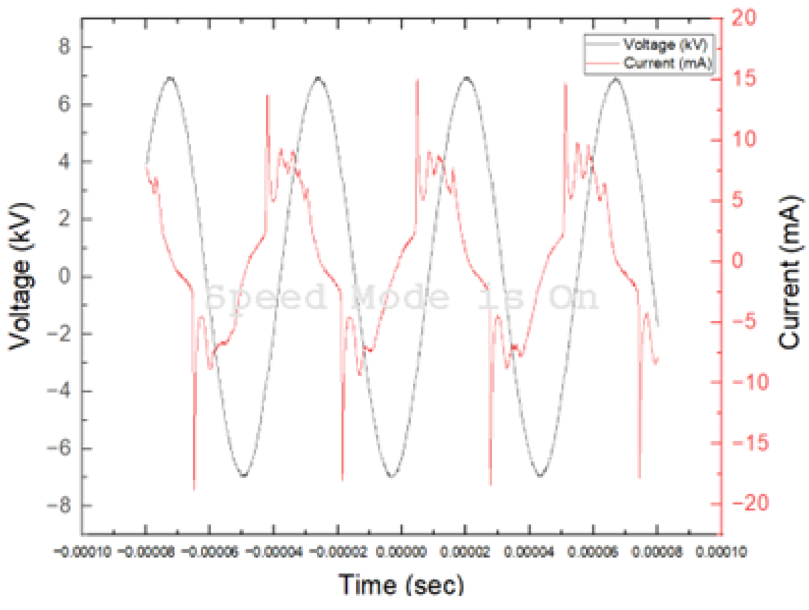

Figure 3. Current voltage graph.

2251-7227[https://doi.org/10.57647/j.jtap.2025.1904.37]

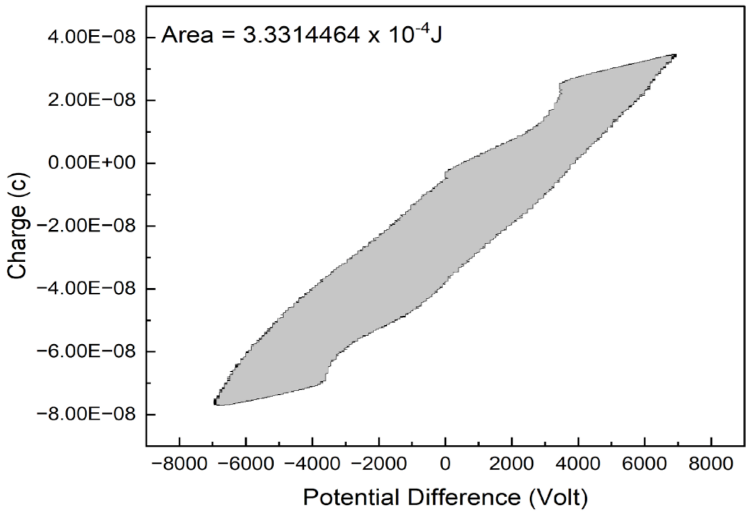

Figure 4. Lissajous Figure.

3.2 Optical characterization

Optical emission spectroscopy is extensively utilized for low temperature plasma diagnostics [34]. This approach is non-intrusively adaptable and comparably affordable. Electron density and temperature may be calculated using the line intensity ratio technique. The intensity of each spectral line is determined by the number density of gas species in the higher state, and each spectral line corresponds to an optical transition between two quantum states of an atom. The temperature and density of electrons determine the number density.

3.2.1 Line intensity ratio method

The species present in the spectra is given in Table 1. These species are identified according to National Institutes of Standard and Technology (NIST) atomic database. Four suitable lines (two for Ar I, and two for Ar II) are chosen from the spectra and the electron temperature T_e is determined using the line intensity ratio method by using the formula [35]

$$\frac{R_1}{R_2} = \frac{\frac{I_1}{I_2}}{\frac{I_3}{I_4}} = (\frac{A_{pq}}{A_{rs}})(\frac{g_p}{g_q})(\frac{\lambda_{xy}}{\lambda_{pq}})(\frac{A_{uv}}{A_{xy}})(\frac{g_u}{g_x})(\frac{\lambda_{rs}}{\lambda_{uv}}) \times \exp[-\frac{E_p - E_r - E_x + E_u}{kT_e}] \quad (2)$$

where T_e is the electron temperature, I the spectral line intensity, and R the ratio of two lines' intensities. The transition probability is represented as A_{ij}, $i \to j$, g_i is the higher level's statistical weight, λ is the radiation's wavelength, E_i is the upper level's energy, and k is the Boltzmann constant. The observation provides the values of λ and I, while the National Institutes of Standards and Technology (NIST) database provides the values of A_{ij}, g_i, and E_i.

$$\frac{R_1}{R_2} = 3.6 \times 10^{-2} \exp[\frac{0.972}{KT_e}] \quad (3)$$

A typical optical emission spectra of atmospheric pressure argon plasma jet generated at 7 kV with frequency 27 kHz is shown as in Fig. 5. It infers the presence of different species in the plasm jet. A few Ar I and Ar II lines with their corresponding values are given in Table 1. This data is taken from NIST Database.

Figure 6 shows the variation of intensity ratio with electron temperature. From this graph, it was found that the electron temperature was 0.365 eV. The average kinetic energy of electrons in a system is referred to as the electron temperature, which is a measurement of the thermal energy of electrons at a specific temperature. The average kinetic energy per electron is expressed in electron volts by this number.

3.2.2 Stark broadening method

Understanding the physical and chemical processes of plasma requires knowledge of the electron temperature and density. Electron density is measured using the Spectral

Table 1. Intensity and wavelength of Ar I and Ar II lines at 7 kV.

Lines	Wavelength (nm)	Transition probability (S^{-1})	Statistical weight	Energy (eV)	Intensity (au) at 7 kV
Ar I	$\lambda_{pq} = 696.80$	$A_{pq} = 6.4 \times 10^6$	$g_p = 3$	$E_p = 13.327$	$I_1 = 3252.48$
Ar I	$\lambda_{rs} = 750.70$	$A_{rs} = 4.5 \times 10^7$	$g_r = 1$	$E_r = 13.479$	$I_2 = 1611.37$
Ar II	$\lambda_{xy} = 338.08$	$A_{xy} = 1.9 \times 10^8$	$g_x = 4$	$E_x = 23.630$	$I_3 = 7422$
Ar II	$\lambda_{uv} = 381.69$	$A_{uv} = 1.7 \times 10^7$	$g_u = 4$	$E_u = 22.81$	$I_4 = 2134$

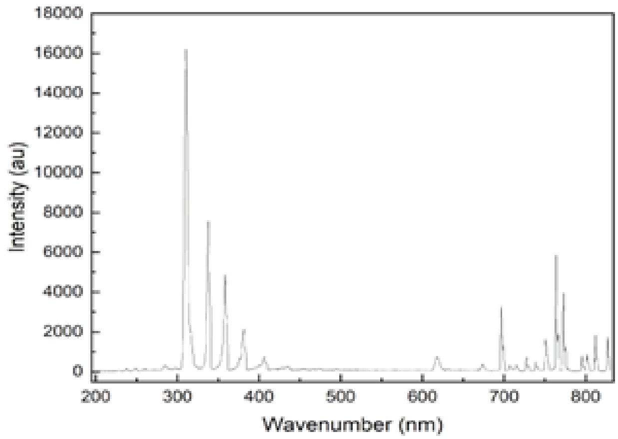

Figure 5. Optical emission spectrum of the discharge at 7 kV with frequency 27 kHz.

Line Profile Method, Laser Thompson Scattering, and the Langmuir probe. However, Laser Thompson Scattering is a sophisticated technique, and Langmuir probes work well with low pressure plasma. The spectral line profile approach works well because of its straightforward equipment and non-instructive features.

In plasma, the electron density exceeds 10^{15} cm^{-3}. Thus, the stark impact is significant, and as a result, stark broadening is employed in plasma diagnostic application. Sharp broadening results from atoms' coulomb interactions with charged particles in plasma. Neutral broadening's full width at half maximum (FWHM) $\Delta\lambda_{\text{strak}}$ (nm) depends on electron temperature T_e (K) and electron density n_e (cm^{-3}).

$$\Delta\lambda_{\text{stark}} = 2 \times 10^{-11} n_e^{\frac{2}{3}} \tag{4}$$

The stark profile is described by the sum of these two asymmetrical Lorentzian Spectral Line profile because of plasma ions impact broadening [35]. The electron density was also calculated using Stark Broadening Method [36, 37].

The argon line at 696.85 nm was selected for this. Fig. 7 displays the Lorentzian fit of the data. The electron density is connected to the full width at half maximum (FWHM) of stark broadening $\Delta\lambda_{\text{stark}}$ by equation (3).

The valve of $\Delta\lambda_{\text{stark}}$ is 2.34 nm and electron density were found to be 3.99×10^{16} cm^{-3}.

3.3 FTIR analysis of radish

A sample's chemical makeup and one of its functional groups can be inferred from the FTIR spectrum. A FTIR spectrum's transmittance shows how much light was absorbed at each frequency. A collection of atoms in a molecule having unique chemical characteristics is called a functional group. A high transmission at a certain frequency indicates that the sample has few bonds to absorb that color light. The functional groups in a sample can be located and measured using the transmittance spectrum.

Equal-sized seeds were collected for FTIR. Fig. 8 displays the FTIR of the treated and untreated seeds. In relation to wavenumber transmittance, the seeds' transmittance rises. It was found that as the wavenumber grows, so does the

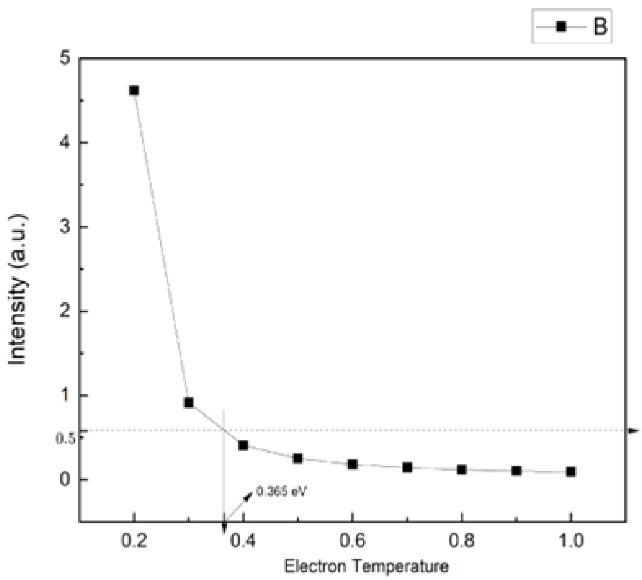

Figure 6. R_1/R_2 as function of electron temperature.

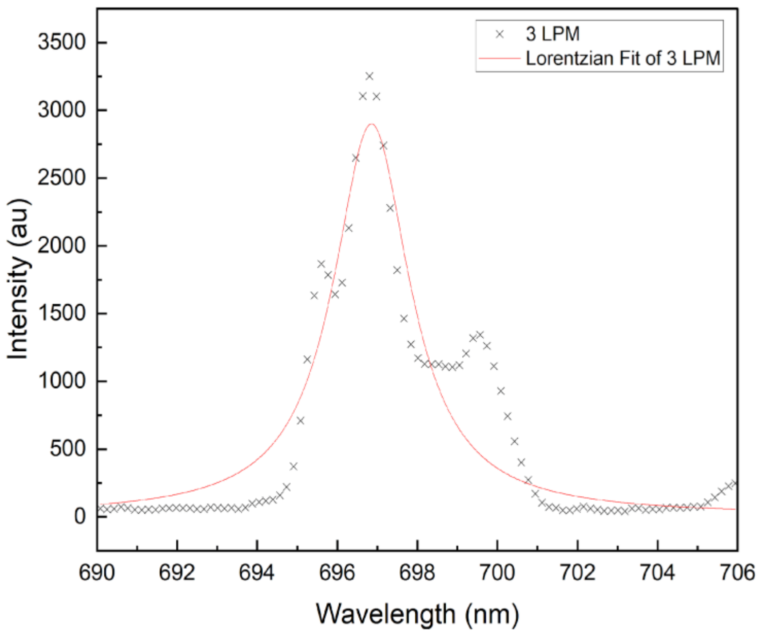

Figure 7. Spectrum of the discharge at 5 kV with frequency 27 kHz.

transmittance. Table 1 displays the functional group identification. The transmittance was seen to change with treatment time. The rate rises for 2.5 and 3 minutes but falls after 30 seconds, 1 minute, 1.5 minutes, and 2 minutes. A drop in transmittance at a certain wavelength indicates a rise in the functional group's concentration, whereas an increase in transmittance indicates a decrease in the concentration at that wavenumber. This study suggests that the plasma treatment affects functional group of seeds which might change growth and development.

From Table 2, at (2914-2925), the transmittance rises for 2.5 and 3 minutes and falls for 30 seconds, 1 minute, 1.5 minute, and 2 minutes treated seeds. It indicates that the concentration of the C-H functional group rises in seeds treated for 30 seconds, 1 minute, 1.5 minutes, and 2 minutes, and falls in seeds treated for 2.5 minutes and 3 minutes.

Transmittance in treated seeds reduces for 30 seconds, 1 minute, 1.5 minute, and 2 minutes compared to untreated seeds at 1745–1746, but rises for 2.5 and 3 minutes. It shows that the C=O group rises in treated seeds for up to two minutes, but then falls for two and three minutes [38].

The transmittance of treated seeds drops during 30 seconds, 1 minute, 1.5 minutes, and 2 minutes at (1463–1466), although it drops for 2.5 minutes and 3 minutes. It shows

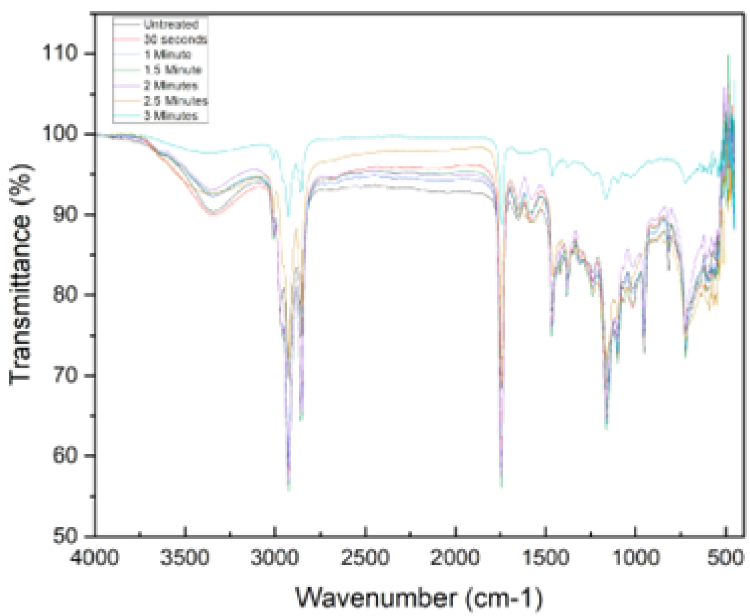

Figure 8. FTIR of radish.

Table 2. Wavenumber and transmittance of radish.

Absorption peak wavenumber (cm^{-1})	Functional group	Transmittance %						
		Untreated	30 sec	1 min	1.5 min	2 min	2.5 min	3 min
2914 - 2925	C-H	70	58	59	64	55	72	90
1745 - 1746	C=O	68	60	58.5	57	55	69	89
1463 - 1466	C-H	81	76	75	75	74	82	95

that treated seeds had higher concentrations of C-H bending. between 30 seconds, 1 minute, 1.5 minutes, and 2 minutes, it stays about the same in treated seeds; however, between 2.5 and 3 minutes, C-H bending diminishes in treated seeds.

3.4 Germination

Radish (Raphanus Sativus)

The untreated and treated radish seeds were sowed. The number of germinations were counted every day, After 20 days, area of leaf, chlorophyll content, and shoot length were measured.

The radish seeds' germination rate, mean germination time and germination index were all assessed [39]. Figure 9 shows a typical glimpse of germination of radish seeds at different treatment time with and without plasma discharge.

3.4.1 Germination rate

The germination rate of seeds is the number of seeds that germinate over a specific number of days. The germination rate was found by using:

$$\text{Germination Rate (G.R.)} = \frac{100(n_1 + n_2 + \cdots + n_i)}{N} \quad (5)$$

where n_1 is the total number of seeds germination on first day, n_2 is the total number of seeds germinated on 2^{nd} day, n_i is the total number of seeds germinated on the i^{th} day, and N is the total number of seeds sown.

Figure 10 shows the germination rates for untreated, 30-second, 1-minute, 1.5-minute, 2-minute, 2.5-minute, and 3-minute treated seeds were 74%, 90%, 84%, 88%, 92%, 64%, and 54%, respectively. The viability of a population of seeds is estimated by seed germination.

This result reveals that the rate of germination of seeds increases for 30 second, 1 minute, 1.5 minute, and 2 minutes respectively, but decreases for 2.5 minutes and 3 minutes plasma treatment.

3.4.2 Mean germination time

The mean germination time shows how quickly the seeds germinate on average. The mean germination time was found by using the formula:

$$\text{Mean Germination Time (MGT)} = \frac{\Sigma(n \times d)}{N} = \frac{n_1 d_1 + n_2 d_2 + \cdots + n_i d_i}{N} \quad (6)$$

where $n_1, n_2, \cdots, n_i$ stands for number of seeds germinated on first day, second day and ith day, $d_1, d_2, \cdots, d_i$ denotes first day, second day and i^{th} day respectively, and N denotes the total number of seeds germinated on test day. It was found to be 8.43, 8.17, 8.11, 6.90, 6.67, 7.62, 6.88 for Untreated, 30 second, 1 minute, 1.5 minutes, 2 minutes, 2.5 minutes and 3 minutes treated seeds respectively.

The outcome indicates that the mean germination time decreases for 30 second, 1 minute, 1.5 minute and 2 minute plasma treated seed but increases for 2.5 minutes and then decreases for 3 minutes treated seeds.

3.4.3 Germination index (GI)

The most often used metric to assess the rate and consistency of seed germination is the germination index (GI). It provides a more understandable indicator of seed vigor than just counting the number of seeds that germinated by combining germination speed and germination percentage. Faster and more consistent germination is measured by a higher GI. The following formula was used to get the germination index (GI):

$$\text{G.I.} = \sum \frac{G(t)}{D(t)} = \frac{G_1}{D_1} + \frac{G_2}{D_2} + \cdots + \frac{G_i}{D_i} \quad (7)$$

where $G_1, G_2, \cdots, G_i$ are the total number of germinations on first day, second day and on ith day, and $D_1, D_2, \cdots, D_i$ indicate the 1^{st} day, 2^{nd} day and i^{th} day respectively.

For untreated, 30 second, 1 minute, 1.5 minutes, 2 minutes, 2.5 minutes, and 3 minutes treated seeds, the corresponding values were 4.87, 5.45, 6.46, 6.66, 7.53, 4.53, and 4.13 as shown in Fig. 11.

Figure 12 refers that the germination index for plasma treated seeds upto 2 minutes and after then it decreases up to 3 minutes.

As a result, it was discovered that treated seedlings had higher germination parameters after two minutes of plasma treatment. The germination characteristics are reduced by higher plasma dosages for 2.5 and 3 minutes.

3.4.4 Effect of NTP on plant shoot length

The bar graph showing in Fig. 13 quantitatively represents the effect of non-thermal plasma treatment duration on plant shoot length. Length measurements, presented with standard error bars, indicate a progressive enhancement in shoot elongation from the untreated condition up to 2 minutes of plasma exposure. Specifically, there is a noticeable increase in shoot length from approximately 17.2 cm (untreated) to a peak near 18 cm at the 2-minutes treatment, suggesting that plasma-induced reactive species may stimulate cellular division and elongation processes within the plant meristematic tissue during this period. However, beyond this

Untreated

30 seconds

1 Minute

1.5 Minutes

2 Minutes

2.5 Minutes

3 Minutes

Figure 9. Germination of radish seed.

2251-7227[https://doi.org/10.57647/j.jtap.2025.1904.37]

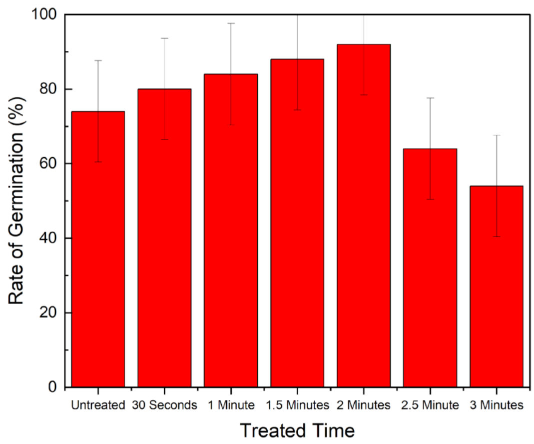

Figure 10. Rate of germination of radish.

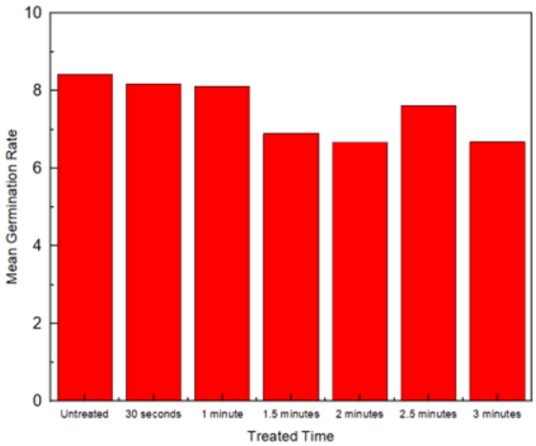

Figure 11. Mean germination time of radish.

optimal threshold, a decline is observed at 2.5 and 3 minutes, where shoot length decreases to values below those of the control. This reduction implies that prolonged exposure likely leads to oxidative stress or disruption of hormonal signaling pathways, thereby inhibiting growth. The error bars, although small, confirm the reproducibility of the data across replicates. Overall, the graph supports the hypothesis that plasma treatment exerts a biphasic effect on plant growth, with short-term exposure promoting and long-term exposure suppressing shoot elongation.

3.4.5 Effect of NTP on leaf area of seedling

The bar graph showing in Fig. 14 displays the leaf area (in mm^2) of Left Leaf, Right Leaf, and 1st True Leaf at various plasma treatment duration ranging from untreated to 3 minutes. Initially, leaf area increases with treatment time, reaching a peak at 1.5 to 2 minutes for all three leaf types, indicating that plasma exposure up to this point promotes leaf growth. The 1st True Leaf generally exhibits the largest area compared to the other leaves throughout the treatments. However, beyond 2 minutes of exposure, a sharp decline in leaf area is observed, especially notable at 3 minutes where the Right Leaf shows a drastic reduction. This suggests that while moderate plasma treatment enhances leaf expansion, extended exposure may have detrimental effects on leaf development.

3.4.6 Measurement of change in chlorophyll content

Chlorophyll contents are key indicators of plant health and physiological status. Chlorophyll exists in various forms, with chlorophyll *a* and chlorophyll *b* being the most common types found in photosynthetic plants and green algae. These pigments are primarily responsible for the green coloration of plants, and their concentration significantly influences the plant's chemical composition. As such, pigment content is often used in statistical analyses to assess plant physiology and biochemical characteristics.
In this study, we analyzed the changes in chlorophyll content in plant extracts in relation to different duration of plasma treatment. The bar graph in Fig. 15 illustrates the chlorophyll content (measured in SPAD units) in three types of plant leaves-Left Leaf, Right Leaf, and 1st True Leaf-across different plasma treatment duration ranging from untreated to 3 minutes. Overall, the 1st True Leaf consistently shows the highest chlorophyll content across all treatment times, with a peak around 2 minutes. Both Left and Right Leaves exhibit a gradual increase in chlorophyll content up to 2 minutes of treatment, after which there is a noticeable decline, particularly in the 2.5 and 3-minute treatments. This trend suggests that short plasma exposure (up to 2 minutes) enhances chlorophyll accumulation, especially in the 1st

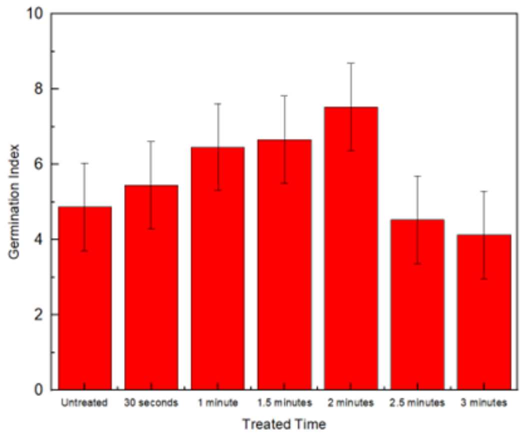

Figure 12. Germination index of radish.

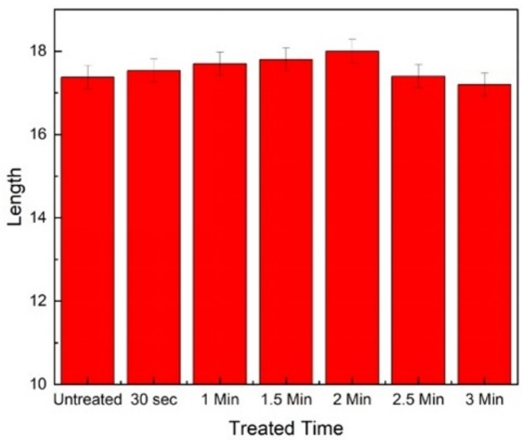

Figure 13. Shoot length of radish as function of treated time.

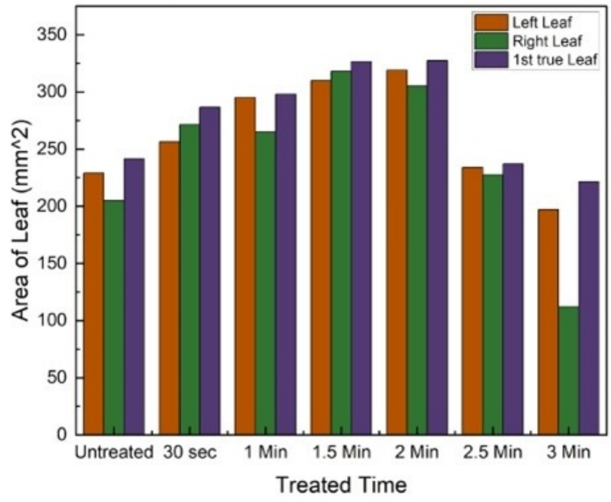

Figure 14. Area of Leaf as function of treated time.

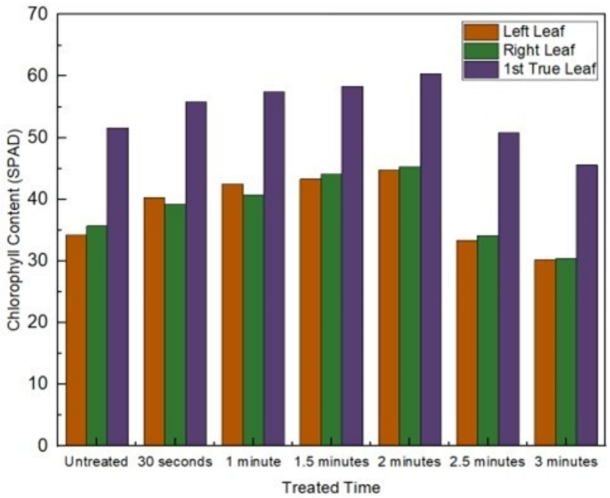

Figure 15. ChlorophyII content in plant with treated time.

True Leaf, while prolonged exposure beyond this threshold negatively impacts chlorophyll levels.

4. Conclusion

A low-cost plasma generation system using locally accessible materials has been created. Both electrical and optical techniques have been used to characterize the plasma jet. By using the stark broadening technique and power balance, the electron density was determined to be around 1.28×10^{17} m^{-3} and 3.99×10^{16} cm^{-3}, respectively. Using the line intensity ratio approach, the electron temperature was determined to be 0.365 eV. Plasma treatment increased the radish seed's germination parameters, leaf area, and shoot length. Additionally, treated seeds have higher levels of chlorophyll. When applied to radish seedlings, the plasma therapy appears to be beneficial for up to two minutes. The rate of germination, shoot length, leaf area, and chlorophyll were all observed to decrease when plasma was applied to seeds for 2.5 and 3 minutes. According to FTIR research, transmittance rises throughout the 2.5 and 3-minute treatment periods and falls during the first two minutes.

Authors Contribution
The intellectual substance, idea, and design of this study, or the analysis and interpretation of the data (if applicable), as well as the manuscript's writing, were all sufficiently contributed to by each author.

Availability of data and materials
The data that support the findings of this study are available from the corresponding author upon reasonable request.

Conflict of interests
The authors declare that they have no known competing financial interests or personal relationships that could have appeared to influence the work reported in this paper.

References

[1] Boyd. T and Sanderson J. "The Physics of Plasma.". *Cambridge University Press*, 2003.

[2] Gomez E., Rani D.A., Cheeseman C.R., Deegan D., Wise M., and Boccaccini A.R. "Thermal plasma technology for the treatment of wastes: A critical review.". 2000.

[3] Hoffmann C, Berganza C, and Zhang J. "Cold Atmospheric Plasma: methods of production and application in dentistry and oncology.". 2010.

[4] Ruj. B and Ghosh. S. "Technological aspects for thermal plasma treatment of municipal solid waste—A review.". 2014.

[5] Samal. S. "Thermal Plasma technology; the prospective in material processing.". 2017.

[6] Laroque. DA, Seo. ST, Valencia. GA, Laurindo. JB, and Carofi. BAM. "Cold Plasma in Food Processing; Design Mechanism and Application.". 2022.

[7] G. Fridman, G. Friedman, A. Gutsol, and et al. "Applied Plasma Medicine.". *Plasma Processes and Polymers*, **5**:503–533, 2008. DOI: https://doi.org/10.1002/ppap.200700154.

[8] M. Šimor, J. Ráhel, P. Vojtek, and et al. "Atmospheric-Pressure Diffuse Coplanar Surface Discharge for Surface Treatments.". *Applied Physics Letters*, **81**:2716–2718, 2002. DOI: https://doi.org/10.1063/1.1513185.

[9] D.B. Graves. "Low Temperature Plasma Biomedicine: A Tutorial Review.". *Physics of Plasmas*, **21**:080901, 2014. DOI: https://doi.org/10.1063/1.4892534.

[10] M.G. Kong, G. Morfill, and W. Stolz. "Plasma Medicine Applications of Low-Temperature Gas Plasmas in Medicine and Biology.". *Cambridge University Press*, 2012.

[11] X. Lu, G.V. Naidis, M. Laroussi, S. Reuter, D.B. Graves, and K. Ostrikov. "Reactive Species in Non-Equilibrium Atmospheric-Pressure Plasmas: Generation, Transport, and Biological Effects.". *Physics Reports*, **630**:1–84, 2016. DOI: https://doi.org/10.1016/j.physrep.2016.03.003.

[12] R.M. France and R.D. Short. "Plasma Treatment of Polymers: The Effects of Energy Transfer from an Argon Plasma on the Surface Chemistry of Polystyrene and Polypropylene. A high-energy resolution X-ray photoelectron study.". *Langmuir*, **14**:4827–4835, 1998.

[13] M. France and R. D. Short. "Plasma treatment of polymers: Effects of energy transfer from an argon plasma on the surface chemistry of poly(styrene), low-density poly(ethylene), poly(propylene), and poly(ethylene terephthalate).". *Journal of the Chemical Society, Faraday Transactions*, **93**(17):3173–3178, 1997. DOI: https://doi.org/10.1039/A702311A.

[14] S. Wild and L.L. Kesmodel. “High Resolution Electron Energy Loss Spectroscopy Investigation of Plasma-Modified Polystyrene Surfaces.”. *Journal of Vacuum Science & Technology A*, **19**:856–860, 2001.
DOI: https://doi.org/10.1116/1.1359531.

[15] U. Lommatzsch, M. Noeske, J. Degenhardt, T. Wübben, S. Strudthoff, G. Ellinghorst, and O.-D. Hennemann. “Pretreatment and Surface Modification of Polymers via Atmospheric-Pressure Plasma Jet Treatment.”. *Polymer Surface Modification: Relevance to Adhesion*, **4**:25–32, 2007.
DOI: https://doi.org/10.1163/ej.9789067644532.i-306.10.

[16] E. Bormashenko, R. Grynyov, Y. Bormashenko, and E. Drori. “Cold Radiofrequency Plasma Treatment Modifies Wettability and Germination Speed of Plant Seeds.”. *Scientific Reports*, **2**:741, 2012.
DOI: https://doi.org/10.1038/srep00741.

[17] M. Selcuk, L. Oksuz, and P. Basaran. “Decontamination of Grains and Legumes Infected with Aspergillus spp. and Penicillum spp. by Cold Plasma Treatment.”. *Bioresource Technology*, **99**:5104–5109, 2008.
DOI: https://doi.org/10.1016/j.biortech.2007.09.076.

[18] P. Basaran, N. Basaran-Akgul, and L. Oksuz. “Elimination of Aspergillusparasiticus from Nut Surface with Low Pressure Cold Plasma (LPCP) Treatment.”. *Food Microbiology*, **25**:626–632, 2008.
DOI: https://doi.org/10.1016/j.fm.2007.12.005.

[19] M. Henselova, L. Slováková, M. Martinka, and et al. “Growth, Anatomy and Enzyme Activity Changes in Zeamays L. Roots Induced by Treatment of Seeds with Low-Temperature Plasma.”. *Biologia*, **67**:490–497, 2012.
DOI: https://doi.org/10.2478/s11756-012-0046-5.

[20] B. Surowsky, A. Fischer, O. Schlueter, and et al. “Cold Plasma Effects on Enzyme Activity in a Model Food System.”. *Innovative Food Science and Emerging Technologies*, **19**:146–152, 2013.
DOI: https://doi.org/10.1016/j.ifset.2013.04.002.

[21] M.Q. Yin, M.G. Huang, B.Z. Ma, and et al. “Stimulating Effects of Seed Treatment by Magnetized Plasma on Tomato Growth and Yield.”. *Plasma Science and Technology*, **7**:3143–3147, 2005.
DOI: https://doi.org/10.1088/1009-0630/7/6/017.

[22] F. Denes, S. Manolache, and R.A. Young. “Synthesis and Surface Functionalization under Cold-Plasma Conditions.”. *Journal of Photopolymer Science and Technology*, **12**:27–38, 1999.
DOI: https://doi.org/10.2494/photopolymer.12.27.

[23] L. Li, J.F. Jiang, J.G. Li, M.C. Shen, X. He, H.L. Shao, and Y.H. Dong. “Effects of Cold Plasma Treatment on Seed Germination and Seedling Growth of Soybean.”. *Scientific Reports*, **4**:5859–5865, 2014.

[24] M. Kanjevac, D. Jakovljević, M. Todorović, M. Stanković, S. Ćurčić, and B. Bojović. “Improvement of Germination and Early Growth of Radish (Raphanus Sativus L.) through modulation of seed metabolic processes.”. 2020.

[25] Y. Xie, L. Xu, Y. Wang, L. Fan, Y. Chen, M. Tang, X. Luo, and L. Liu. “Comparative proteomic analysis provides insight into a complex regulatory network of taproot formation in radish (Raphanus sativus L.).”. 2018.

[26] E.M. Muleke, Y. Wang, W. Zhang, L. Xu, J. Ying, B.K. Karanja, X. Zhu, L. Fan, Z. Ahmadzai, and L. Liu. “Genome-wide identification and expression profiling of MYB transcription factor genes in radish (Raphanus sativus L.).”. 2017.

[27] C.H. Park, T.B. Baskar, S.-Y. Park, S.-J. Kim, M. Valan Arasu, N.A. Al-Dhabi, J.K. Kim, and S.U. Park. “Metabolic Profiling and Antioxidant Assay of Metabolites from Three Radish Cultivars (Raphanus sativus).”. *Molecules*, **21**:157, 2016.
DOI: https://doi.org/10.3390/molecules21020157.

[28] A. Noman, Q. Ali, J. Maqsood, N. Iqbal, M.T. Javed, N. Rasool, and J. Naseem. “Deciphering physio-biochemical, yield, and nutritional quality attributes of water-stressed radish (Raphanus sativus L.) plants grown from Zn-Lys primed seeds.”. 2020.

[29] L. Ling, J. Jiafeng, L. Jiangang, and et al. “Effects of cold plasma treatment on seed germination and seedling growth of soybean.”. *Scientific Reports*, **4**:5859, 2014.
DOI: https://doi.org/10.1038/srep05859.

[30] Y. J. Chou, K. C. Cheng, F. C. Hsu, J. S. Wu, and Y. Ting. “Producing high-quality mung bean sprout using atmospheric cold plasma treatment: Better physical appearance and higher γ-aminobutyric acid (GABA) content.”. *Journal of the Science of Food and Agriculture*, **101**(15):6463–6471, 2021.
DOI: https://doi.org/10.1002/jsfa.11317.

[31] N. Jiang, A. Ji, and Z. Cao. “Atmospheric pressure plasma jet: Effect of electrode configuration, discharge behavior, and its formation mechanism.”. *Journal of Applied Physics*, **106**:013308, 2009.
DOI: https://doi.org/10.1063/1.3159884.

[32] B. K Thakur, A. K. Shah, R. L. Sah, R. Silpakar, Shrestha R, and L. N. Mishra. “Plasma jet therapy on seeds for improvement of germination and development.”. *Int. J. Plasma Environ. Sci. Technol.*, **19**(1):12, 2025.
DOI: https://doi.org/10.34343/ijpest.2025.19.e01001.

[33] M. Teschke, J. Kedzierski, E. G. Finantu-Dinu, D. Korzec, and J. Engemann. “High-speed photographs of a dielectric barrier atmospheric pressure plasma jet.”. *IEEE Transactions on Plasma Science*, **33**(2): 310–311, 2005.
DOI: https://doi.org/10.1109/TPS.2005.845377.

[34] A. Souhaila and A. Rachid. “Spectroscopic analysis of argon plasma for electron temperature determination.”. 2023.
DOI: https://doi.org/10.54021/seesv5n2-724.

[35] N. Balcon, A. Aanesland, and R. Boswell. “Pulsed RF discharges, glow and filamentary mode at atmospheric pressure in argon.”. *Plasma Sources Science and Technology*, **16**(2):217, 2007.
DOI: https://doi.org/10.1088/0963-0252/16/2/002.

[36] Dong. L, Ran. J., and Mao. Z. “Direct measurement of electron density in micro discharge at atmospheric by stark broadening.”. *Applied Physics*, 2015.

[37] A. Falahat, A. Ganjovi, M. Taraz, et al. “Optical characteristics of an RF DBD plasma jet in various Ar/O 2 mixtures.”. *Pramana - Journal of Physics*, **90**:27, 2018.
DOI: https://doi.org/10.1007/s12043-018-1520-6.

[38] H.B. Baniya. “Experimental Study of atmospheric pressure plasma jet (APPJ) with floating electrode and its application for polymer surface modification.”. *M.Phil. Thesis, Kathmandu University*, 2016.

[39] B. Šera. “Methodological contribution on seed germination and seedling initial growth tests in wild plants.”. *Notulae Botanicae Horti Agrobotanici Cluj-Napoca*, **51**(2):13164, 2023.